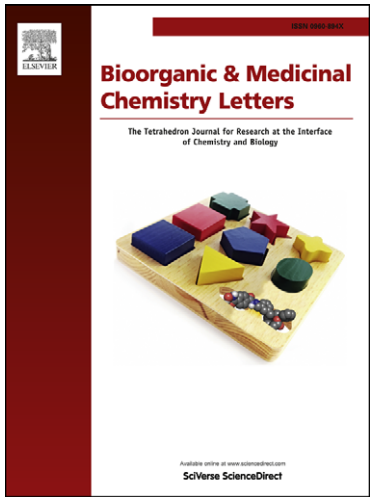

Design, synthesis and structure-activity relationships of 3,5-diaryl-1*H*-pyrazoles as inhibitors of arylamine *N*-acetyltransferase

Elizabeth Fullam, James Talbot, Areej Abuhammed, Isaac Westwood, Stephen G. Davies, Angela J. Russell, Edith Sim

PII: S0960-894X(13)00228-X
DOI: http://dx.doi.org/10.1016/j.bmcl.2013.02.052
Reference: BMCL 20170

To appear in: *Bioorganic & Medicinal Chemistry Letters*

Received Date: 11 December 2012
Revised Date: 8 February 2013
Accepted Date: 12 February 2013

Please cite this article as: Fullam, E., Talbot, J., Abuhammed, A., Westwood, I., Davies, S.G., Russell, A.J., Sim, E., Design, synthesis and structure-activity relationships of 3,5-diaryl-1*H*-pyrazoles as inhibitors of arylamine *N*-acetyltransferase, *Bioorganic & Medicinal Chemistry Letters* (2013), doi: http://dx.doi.org/10.1016/j.bmcl.2013.02.052

Design, synthesis and structure-activity relationships of 3,5-diaryl-1*H*-pyrazoles as inhibitors of arylamine *N*-acetyltransferase[†]

Elizabeth Fullam,*[abc] James Talbot,[ab] Areej Abuhammed,[ad] Isaac Westwood,[abe] Stephen G. Davies,[b] Angela J. Russell,[ab] Edith Sim*[ae]

[a]*Department of Pharmacology, University of Oxford, Mansfield Road, Oxford, UK, OX1 3QT.*
[b]*Department of Chemistry, Chemistry Research Laboratory, University of Oxford, Mansfield Road, Oxford, UK, OX1 3TA.*
[*c] *Current address School of Life Sciences, Gibbet Hill Campus, The University of Warwick, Coventry, CV4 7AL, United Kingdom. E-mail e.fullam@warwick.ac.uk Tel +44 (0)24 765 74251*
[d] *Faculty of Pharmacy, University of Jordan, Queen Rania Street, Amman 11942, Jordan*
[e]*Current address Institute of Cancer Research, Chester Beatty Laboratories, 237 Fulham Road, London SW3 6JB.*
[e] *Current address Faculty of Science, Engineering and Computing Kingston University, Penrhyn Road, Kingston KT1 2EE, UK. E-mail e.sim@kingston.ac.uk*

[*]*Corresponding authors: Elizabeth Fullam:* email *e.fullam@warwick.ac.uk Tel +44 (0)24 765 74251* and Edith Sim: *email e.sim@kingston.ac.uk Tel +44 (0)20 8417 2492*

[†]Electronic Supplementary information (ESI) available: Experimental data for compounds 1 to 32 and materials and methods for *in vitro* assays

The synthesis and inhibitory potencies of a novel series of 3,5-diaryl-1*H*-pyrazoles as specific inhibitors of prokaryotic arylamine *N*-acetyltransferase enzymes is described. The series is based on hit compound **1** 3,5-diaryl-1*H*-pyrazole identified from a high-throughout screen that has been carried out previously and found to inhibit the growth of *Mycobacterium tuberculosis*.

Graphical Abstract

FIGURE UPLOADED SEPARATELY

A series of novel 3,5-diaryl-1*H*-pyrazoles inhibitors were synthesized and evaluated as inhibitors of prokaryotic arylamine *N*-acetyltransferase enzymes.

Tuberculosis (TB) remains the single most important bacterial cause of morbidity and mortality in the world. *Mycobacterium tuberculosis* is the causative agent of TB and in 2010 TB infection resulted in an estimated 1.4 million deaths worldwide (http://www.who.int/tb/publications/global_report/2011/en/). The TB bacillus currently infects one-third of the world's population and in 2010 alone 8.8 million new cases of TB were reported [1, 2]. Treatment for TB is complicated and requires that at least three drugs be taken concomitantly for six to nine months, often with unpleasant side effects. The long treatment time, coupled with patient non-compliance has led to the emergence of multi-drug resistant (MDR) and extensively drug-resistant (XDR-TB) strains of TB that further complicates treatment. Staggeringly, the number of reported MDR cases has increased from 150,000 in 2008 to 650,000 in 2010. More recently, totally drug-resistant (TDR-TB) strains of TB have emerged for which there are no successful chemotherapy regimens. The *M. tuberculosis* cell envelope structure is rich in polysaccharides and lipids and accounts for its unusual low permeability towards commonly used antibiotics, contributing to its resistance [3-5]. In combination with immuno-compromised individuals with HIV, TB represents a serious health problem. Consequently there is a dire need for new drugs to treat TB [6].

Biosynthetic pathways that are present in the pathogen *M. tuberculosis* and not present in the human host represent an approach to identifying specific targets for TB therapy [7, 8]. A unique pathway, comprising a five gene operon (*Rv3570c-Rv3566c),* that is involved in complex cell wall lipid biosynthesis and cholesterol catabolism in *M. tuberculosis* has been identified and characterized [9-11]. These genes have been shown to be upregulated in microarray studies [12, 13]. Single gene, genetic knockouts of *hsaD*, *hsaA* and *nat* have shown that these enzymes are essential for the intracellular survival of *M. tuberculosis* in macrophages [10, 11, 14-19]. The *nat* gene in *M. tuberculosis* is the last gene in this cluster and the *N*-acetyl transferase (NAT) enzyme can

catalyse the hydrolysis of both *n*-propionyl Coenzyme A, a product of cholesterol catabolism, as well as the cofactor acetyl Coenzyme A [9, 16]. Deletion of *nat* from *Mycobacterium bovis* BCG (*Δnat)* affects the cell wall composition and the biosynthesis of mycolic acids [10]. Therefore NAT has been implicated as a potential anti-tubercular target for the development of inhibitors [10]. Importantly, X-ray structures of the NAT enzyme are available to assist in the design of inhibitors [20]. Although there is no reported NAT structure from *M. tuberculosis* (TBNAT), the NAT enzyme from *M. marinum* (MMNAT) is 73% identical and 83% similar to the TBNAT at the amino acid level. The MMNAT structure is known with cofactor and substrate bound [21, 22] and whilst not identical to the TBNAT enzyme, has been shown to serve as a suitable model [16, 23].

In previous work, we undertook a high-throughput screen of 5,000 drug-like compounds to find inhibitors of NAT enzymes [24]. From this screen, compounds of distinct structural classes were characterised that were specific inhibitors of either prokaryotic or eukaryotic NAT enzymes [25-27]. In this study we focus on the hit compound 4-methoxy-2-(5-(4-methoxyphenyl)-1*H*-pyrazol-3-yl)phenol **1** identified from the screen **(Fig 1),** a specific inhibitor of prokaryotic NAT enzymes. Here we report on the synthesis of a focused sub-library of 3,5-diaryl-1*H*-pyrazoles that have been designed and synthesised based on predicted interactions of pyrazole **1** with MMNAT. We have evaluated the activities of the sub-library for inhibition of MMNAT enzymic activity. Our data reveal insights into inhibitor-MMNAT interactions and have allowed us to identify key structural motifs within the 3,5-diaryl-1*H*-pyrazole scaffold that play an essential role in inhibition of NAT activity.

The 3,5-diaryl-1*H*-pyrazole moiety identified represents a novel scaffold that had not been identified previously as an inhibitor of NAT enzymic activity. Pyrazole **1,** Figure 1, was deemed to be a promising starting point for lead discovery in terms of predicted physicochemical properties, drug-likeness [28] and chemical tractability: retrosynthetic analysis of the target

compound identified a synthetic route with the potential to modify the scaffold and provide diversification on both aryl-rings around the heterocyclic core depending on the starting material selected. Furthermore, importantly, hit compound **1** was found to have good anti-mycobacterial activity and inhibited the growth of both *M. tuberculosis* and *M. bovis BCG* on solid agar with an MIC <10μg/mL (34μM) [24].

Given the importance of verifying the chemical identity of lead compounds emerging from high-throughput screening [29], pyrazole **1** was resynthesised prior to embarking on the synthesis of a focused sub-library of pyrazole compounds. Pyrazole **1** was resynthesised from commercially available 2'-hydroxy-5'-methoxyacetophenone *via* a crossed-Claisen-type reaction with subsequent condensation with hydrazine to form the required pyrazole moiety, Scheme 1 [30, 31]. The intermediate 1,3-diketone was formed as a mixture with its corresponding enol tautomers. This mixture was not purified and was reacted directly with hydrazine hydrate. Characterisation of the resynthesised pyrazole by ^{1}H and ^{13}C NMR, along with mass spectrometry and elemental analysis confirmed that pyrazole **1** was identical to the hit compound from the screening library [32]. Furthermore resynthesised pyrazole **1** was tested against the NAT enzyme from *P. aeruginosa* (PANAT) used in the initial screen and found to have an IC_{50} of 9.7±0.3μM as an inhibitor of the PANAT enzyme. Hit compound **1** was thus verified as a starting point for further investigation. The NAT enzyme from *M. marinum* is more similar in sequence to the TBNAT enzyme than the NAT enzymes used in the initial high-throughput screen [22, 23]. Therefore, pyrazole **1** was tested for inhibition against MMNAT and found to be a competitive inhibitor with high affinity for MMNAT with a K_i *of* 23μM (SI, Figure 1).

To guide the synthesis of a focused sub-library of 3,5-diaryl-1*H*-pyrazole compounds, docking simulations were performed to obtain structural insights into the binding mode of **1** with

MMNAT, using GOLD [33]. The modelled results suggest that pyrazole **1** binds in the active-site pocket of MMNAT, within 4Å of the γS of the active-site Cys70, part of the Cys-His-Asp active-site catalytic triad of NAT enzymes (Fig 2A). The predicted binding mode and location of **1** has a high degree of similarity with solved NAT structures with substrate bound: MMNAT with CoA (pdb 2vfc) [22] (Fig 2B), MMNAT with hydralazine (pdb 3ltw) [21] (Fig 2C) and MSNAT with isoniazid (pdb 1wf6) [34] (Fig 2D). An overlay of the modelled results of **1** with the solved HDZ-MMNAT, INH-MSNAT and CoA-MMNAT structures indicates that the aryl substituent at C(3) of pyrazole **1** is directly positioned in the same location as the arylhydrazine substrates: the benzene ring of HDZ and the pyridine of isoniazid. The 5'-methoxy group of the aryl substituent at C(3) of pyrazole **1** group points towards the γS of the active-site Cys70 in a similar manner to the terminal nitrogen of the hydrazyl group of isoniazid and hydralazine, which is acetylated by Cys70 in the acetyltransferase reaction. The aryl substituent at C(5) of pyrazole **1** is predicted to extend by a distance of some 8.5Å beyond the arylamine substrate binding site pocket towards the P-loop (residues Gly129, Phe130, Gly131, Gly132) into the cofactor CoA binding site in MMNAT. Consequently, it is envisaged from the modelling studies that inhibition of the MMNAT enzyme is achieved by precluding direct access of NAT substrates and the cofactor acetyl CoA to the active-site of MMNAT thereby preventing the NAT reaction from occurring (Fig 3). These modeling studies are in agreement with the kinetic data that indicate pyrazole **1** is a competitive inhibitor of MMNAT.

Detailed analysis of the molecular contacts predicted from the modelling studies between pyrazole **1** with MMNAT reveal that the majority of interactions are hydrophobic (Fig2A). The 3-aryl substituent within pyrazole **1** is predicted to bind in the hydrophobic pocket formed by residues Phe38, Phe130 and Phe204 that form a lid over the active-site Cys70 with π-stacking interactions between the 3-aryl substituent and Phe130. There is an additional hydrophobic

interaction between this 3-aryl substituent and Val95. The docking studies suggest that the 5'-methoxy group of the 3-aryl substituent is in close proximity (3.7Å) to potentially form a hydrogen bond with the backbone carbonyl of Thr109. Thr109 has been demonstrated previously to be important in substrate binding and recognition of NAT substrates [21, 34]. The backbone carbonyl group of Thr109 forms a hydrogen-bond with the hydrazyl group of HDZ or INH in the MMNAT-HDZ and MSNAT-INH structures respectively [34, 35]. Interestingly, only one hydrogen-bond is predicted between pyrazole **1** and MMNAT, between the 2'-hydroxy group of the 3-aryl substituent and the backbone carbonyl group of P-loop residue Gly131. Although the MMNAT-CoA structure (pdb 2vfc) shows that this P-loop residue is not directly involved in binding to CoA (P-loop residues Phe130 and Gly132 are involved), binding of pyrazole **1** at this site would block the binding of the cofactor acetyl CoA. The 5-aryl substituent extends beyond the P-loop and binds in a second hydrophobic pocket formed by Trp97 and Met209 and Met222. The side-chain of Trp97 is involved in the recognition of the bridging phosphate group of CoA and forms a hydrogen-bond from the indole nitrogen to a phosphate moiety in CoA, therefore this interaction potentially further interrupts binding of CoA to MMNAT. Therefore, the docking studies suggest a number of binding interactions between pyrazole **1** and MMNAT that prevent NAT substrates and the cofactor from binding.

Based on these docking results R^1, R^2, R^3 and R^4 (Table 1) were selected for rational systematic modification to incorporate -H/-F/-OH/-OMe structural modifications into the design of the inhibitor with the aim of investigating the predicted role of the electrostatics, polar moieties and hydrogen bonding between pyrazole **1** and MMNAT. The focused array of pyrazoles was synthesized following an optimization of the synthetic route to target compound **1**: the mixed Claisen-type condensation reactions of arylmethylketones were heated in order to drive formation of the diketone intermediate [31, 36]. Intermediate 1,3-diketones were synthesized from commercially available arylmethylketones and arylcarbonyl chlorides and the reactions

proceeded in good yields. The attempted synthesis of pyrazoles **3** and **4** *via* treatment of the corresponding dihydroxy-substituted ketones with hydrazine hydrate gave a complex mix of products from which **3** and **4** could not be isolated. This was postulated to be due to deprotonation of the acidic phenolic-OH groups under the reaction conditions. Therefore pyrazoles **3** and **4** were synthesised by an alternative route involving protection of the phenol groups within the starting arylmethylketones as the corresponding TBDMS ethers. The *O*-TBDMS protected arylmethylketones were next treated with LiHMDS and the requisite acyl chloride, deprotected *via* treatment with tetrabutylammonium fluoride and the crude reaction mixtures subsequently treated with hydrazine hydrate (Supplementary information, Scheme 1). This resulted in the parallel production of an array of fifteen pyrazoles **2-16** in good overall yields.

To determine SARs for the 3,5-diaryl pyrazole class of heterocycles, the fifteen compounds that formed the sub-library were tested for their inhibitory properties against the MMNAT enzyme. Initially, the compounds were tested at a final concentration of 30μM as inhibitors in a reaction where MMNAT catalysed the acetylation of isoniazid as measured by the hydrolysis of 5,5'-dithiobis-(2-nitrobenzoic acid) (DTNB), as described previously [37]. The synthesized sub-library showed a range of inhibitory activities against MMNAT, from 15% inhibition of MMNAT enzymic activity up to 66% inhibition at 30μM, Table 1. Half maximal inhibitory concentrations (IC_{50}) were determined for the five most potent inhibitors. Testing the analogues of **1** for inhibition of MMNAT has allowed for the derivation of key structural features and preliminary SARs for the library of 3,5-diaryl-1*H*-pyrazole compounds.

Of the fifteen compounds tested, seven compounds were found to have reduced potency at 30μM compared to the initial hit pyrazole **1** at the same concentration**: 2** (29%), **3** (21%), **4** (15%), **6** (26%), **9** (26%), **15** (18%) and **16** (29%). Comparison between the initial hit compound **1** and its

unsubstituted analogue **6** shows a significant decrease in inhibition of MMNAT indicating that the functional groups of hit compound **1** play a positive role in the binding of 3,5-diaryl-1*H*-pyrazole compounds to MMNAT. Intriguingly, the docking studies predicted that the 2'-hydroxy group of the aryl substituent at C(3) of pyrazole **1** forms a hydrogen bond to the backbone carbonyl group of Gly131. Altering the 2'-hydroxy group to a 2'-methoxy group, whilst keeping the remaining functionalities the same (pyrazole **2**) results in a dramatic decrease in the inhibition of MMNAT suggesting the importance of the –OH hydrogen bond donor properties of the 2'-hydroxy group of **1** for MMNAT inhibition. In addition, the hydroxy group is required to be positioned at the 2'-position of the 3-aryl substituent. When the hydroxyl group is orientated at the 3'-position (pyrazole **4**) a decrease in inhibition of MMNAT is also observed (Table 1). The modelling studies predict a number of electrostatic interactions between the 3-aryl substituent within **1** and a hydrophobic pocket formed by three phenylaniline residues: Phe38, Phe130 and Phe204. When the 5'-methoxy group is replaced by a 5'-hydroxy group (pyrazole **3**) the inhibition of MMNAT is greatly reduced with an IC_{50} greater than 30μM. Furthermore, when R^1 and R^3 are substituted to F groups: pyrazole **15**, the same reduction in IC_{50} value is observed. This suggests that the pyrazole compounds do bind in a hydrophobic pocket in MMNAT as predicted from the docking studies and that more hydrophobic groups on the 3-aryl substituent are preferred when R^4 remains a methoxy group. This is consistent with previous studies that have shown that NAT enzymes prefer lipophilic substrates [37].

Of the fifteen compounds synthesised, it was very encouraging that five compounds inhibited the activity of the MMNAT enzyme at 30μM by greater than 50%: compounds **7**, **8**, **10, 11,** and **14**, Table 1, with IC_{50} values of 12.9μM, 21.3μM, 17.6μM, 11.7μM and 18.8μM respectively. A wide-range of functionality at R^4 can be well tolerated and cause good inhibition of MMNAT. Interestingly, two of the most potent inhibitors of MMNAT enzymic activity: **7** and **11** (IC_{50} of

12.9μM and 11.7μM respectively) both have unfunctionalised 5-phenyl substituents, suggesting that functionality on the 3-aryl substituent is more important than functionalisation of the 5-aryl substituent for improving inhibition of MMNAT enzymic activity. It is possible that pyrazoles **7** and **11** have a different mode of binding to MMNAT as a result of the unfunctionalised 5-phenyl substituent and docking studies suggest that pyrazoles **7** and **11** can bind in a 'flipped' orientation to MMNAT (Fig 4) compared to the hit compound **1**, in which the 5-aryl substituent is located in the active-site pocket in close proximity to Cys70. As a result of the predicted "flipped" orientation of **7** and **11** the pyrazole moiety is orientated to point towards the P-loop of MMNAT with the potential to form an additional hydrogen-bond from N(2) of the heterocyclic pyrazole core to the backbone carbonyl group of Gly131 (Fig 5) and may go some way to understanding the improved inhibitory properties of these compounds in the first instance.

In conclusion we have proposed binding modes for a focused library of 3,5-diarylpyrazoles to the mycobacterial NAT enzyme, MMNAT. *In silico* docking studies and analysis of the inhibition data from the sub-library of **1** with MMNAT has allowed for the elucidation of key structural features for the 3,5-diaryl pyrazoles, which are most important for inhibition of MMNAT enzymic activity. Analysis of the binding mode of this library of compounds suggest that the 3,5-diarylpyrazoles are able to bind in the active-site, hydrophobic pocket of MMNAT, stabilised by a number of hydrophobic interactions in a manner that precludes substrate and cofactor from binding. Key hydrogen bonding interactions are predicted to occur between the 3,5-diarylpyrazole scaffold and Gly131 and Thr109, which is further supported by the kinetic data and preliminary SAR analyses. We have identified that the hydrophobic groups on the 3-aryl substituent improve potency and that the most potent inhibitors in the sub-library have unfunctionalised 5-phenyl substituents. This study provides an important insight into the key structural features of this class of compound that inhibits NAT activity that will contribute to

future improvement of potency that can be accomplished by structural modifications to optimize these identified key interactions. A number of pyrazole compounds have been reported to have anti-tubercular activity [38, 39] and here we report that hit compound **1** inhibits the growth of *M. tuberculosis* and *M. bovis* BCG with an MIC of less than 10μg/mL and also inhibits NAT enzymic activity. Anti-tubercular agents are urgently needed and the resulting low-molecular weight, drug like pyrazole compounds presented here represent promising candidates to be further optimized for TB therapy.

Supporting information

Experimental details can be found in the Supporting Information.

Acknowledgements

We would like to thank Hilary Long for excellent technical assistance. We are also grateful to the University of Jordan for a studentship (A.A.).

References and notes

1. Das, P.; Horton, R. *Lancet* **2010,** *375*, 1755.
2. Dye, C. *Lancet* **2006,** *367*, 938.
3. Brennan, P. J.; Nikaido, H. *Annu. Rev. Biochem.* **1995,** *64*, 29.
4. Briken, V.; Porcelli, S. A.; Besra, G. S.; Kremer, L. *Mol. Microbiol.* **2004,** *53*, 391.
5. Dover, L. G.; Cerdeno-Tarraga, A. M.; Pallen, M. J.; Parkhill, J.; Besra, G. S. *Microbiol. Rev.* **2004,** *28*, 225.
6. Ma, Z.; Lienhardt, C.; McIlleron, H.; Nunn, A. J.; Wang, X. *Lancet* **2010,** *375*, 2100.
7. Cole, S. T.; Brosch, R.; Parkhill, J.; Garnier, T.; Churcher, C.; Harris, D.; Gordon, S. V.; Eiglmeier, K.; Gas, S.; Barry, C. E., 3rd; Tekaia, F.; Badcock, K.; Basham, D.; Brown, D.; Chillingworth, T.; Connor, R.; Davies, R.; Devlin, K.; Feltwell, T.; Gentles, S.; Hamlin, N.; Holroyd, S.; Hornsby, T.; Jagels, K.; Krogh, A.; McLean, J.; Moule, S.; Murphy, L.; Oliver, K.; Osborne, J.; Quail, M. A.; Rajandream, M. A.; Rogers, J.; Rutter, S.; Seeger, K.; Skelton, J.; Squares, R.; Squares, S.; Sulston, J. E.; Taylor, K.; Whitehead, S.; Barrell, B. G. *Nature* **1998,** *393*, 537.
8. Fullam, E.; Pojer, F.; Bergfors, T.; Jones, T. A.; Cole, S. T. *Open Biol* **2012,** *2*, 110026.
9. Anderton, M. C.; Bhakta, S.; Besra, G. S.; Jeavons, P.; Eltis, L. D.; Sim, E. *Mol. Microbiol.* **2006,** *59*, 181.

10. Bhakta, S.; Besra, G. S.; Upton, A. M.; Parish, T.; Sholto-Douglas-Vernon, C.; Gibson, K. J.; Knutton, S.; Gordon, S.; DaSilva, R. P.; Anderton, M. C.; Sim, E. *J. Exp. Med.* **2004,** *199*, 1191.
11. Van der Geize, R.; Yam, K.; Heuser, T.; Wilbrink, M. H.; Hara, H.; Anderton, M. C.; Sim, E.; Dijkhuizen, L.; Davies, J. E.; Mohn, W. W.; Eltis, L. D. *Proc. Natl. Acad. Sci. U.S.A* **2007,** *104*, 1947.
12. Sassetti, C. M.; Boyd, D. H.; Rubin, E. J. *Mol. Microbiol.* **2003,** *48*, 77.
13. Sidders, B.; Withers, M.; Kendall, S. L.; Bacon, J.; Waddell, S. J.; Hinds, J.; Golby, P.; Movahedzadeh, F.; Cox, R. A.; Frita, R.; Ten Bokum, A. M.; Wernisch, L.; Stoker, N. G. *Genome Biol.* **2007,** *8*, R265.
14. Dresen, C.; Lin, L. Y.; D'Angelo, I.; Tocheva, E. I.; Strynadka, N.; Eltis, L. D. *J. Biol. Chem.* **2010,** *285*, 22264.
15. Lack, N.; Lowe, E. D.; Liu, J.; Eltis, L. D.; Noble, M. E.; Sim, E.; Westwood, I. M. *Acta Crystallogr., Sect. F.* **2008,** *64*, 2.
16. Lack, N. A.; Kawamura, A.; Fullam, E.; Laurieri, N.; Beard, S.; Russell, A. J.; Evangelopoulos, D.; Westwood, I.; Sim, E. *Biochem. J.* **2009,** *418*, 369.
17. Lack, N. A.; Yam, K. C.; Lowe, E. D.; Horsman, G. P.; Owen, R. L.; Sim, E.; Eltis, L. D. *J. Biol. Chem.* **2010,** *285*, 434.
18. Rengarajan, J.; Bloom, B. R.; Rubin, E. J. *Proc. Natl. Acad. Sci. U.S.A.* **2005,** *102*, 8327.
19. Yam, K. C.; D'Angelo, I.; Kalscheuer, R.; Zhu, H.; Wang, J. X.; Snieckus, V.; Ly, L. H.; Converse, P. J.; Jacobs, W. R., Jr.; Strynadka, N.; Eltis, L. D. *PLoS Pathog.* **2009,** *5*, e1000344.
20. Westwood, I. M.; Kawamura, A.; Fullam, E.; Russell, A. J.; Davies, S. G.; Sim, E. *Curr. Top. Med. Chem.* **2006,** *6*, 1641.
21. Abuhammad, A. M.; Lowe, E. D.; Fullam, E.; Noble, M.; Garman, E. F.; Sim, E. *Protein & Cell* **2010,** *1*, 384.
22. Fullam, E.; Westwood, I. M.; Anderton, M. C.; Lowe, E. D.; Sim, E.; Noble, M. E. *J. Mol. Biol.* **2008,** *375*, 178.
23. Fullam, E.; Kawamura, A.; Wilkinson, H.; Abuhammad, A.; Westwood, I.; Sim, E. *The Protein Journal* **2009,** *28*, 281.
24. Westwood, I. M.; Bhakta, S.; Russell, A. J.; Fullam, E.; Anderton, M. C.; Kawamura, A.; Mulvaney, A. W.; Vickers, R. J.; Bhowruth, V.; Besra, G. S.; Lalvani, A.; Davies, S. G.; Sim, E. *Protein & Cell* **2010,** *1*, 82.
25. Abuhammad, A.; Fullam, E.; Lowe, E. D.; Staunton, D.; Kawamura, A.; Westwood, I. M.; Bhakta, S.; Garner, A. C.; Wilson, D. L.; Seden, P. T.; Davies, S. G.; Russell, A. J.; Garman, E. F.; Sim, E. *PLoS One* **2012,** *7*, e52790.
26. Russell, A. J.; Westwood, I. M.; Crawford, M. H.; Robinson, J.; Kawamura, A.; Redfield, C.; Laurieri, N.; Lowe, E. D.; Davies, S. G.; Sim, E. *Bioorg. Med. Chem.* **2009,** *17*, 905.
27. Westwood, I. M.; Bhakta, S.; Russell, A. J.; Fullam, E.; Anderton, M. C.; Kawamura, A.; Mulvaney, A. W.; Vickers, R. J.; Bhowruth, V.; Besra, G. S.; Lalvani, A.; Davies, S. G.; Sim, E. *Protein & Cell* **2010,** *1*, 82.
28. Lipinski, C. A.; Lombardo, F.; Dominy, B. W.; Feeney, P. J. *Adv. Drug. Deliver. Rev.* **2001,** *46*, 3.
29. Fullam, E.; Abuhammad, A.; Wilson, D. L.; Anderton, M. C.; Davies, S. G.; Russell, A. J.; Sim, E. *Bioorg. Med. Chem. Lett.* **2011,** *21*, 1185.
30. Daskiewicz, J. B.; Depeint, F.; Viornery, L.; Bayet, C.; Comte-Sarrazin, G.; Comte, G.; Gee, J. M.; Johnson, I. T.; Ndjoko, K.; Hostettmann, K.; Barron, D. *J. Med. Chem.* **2005,** *48*, 2790.
31. Govindaswamy, P.; Mozharivskyj, Y. A.; Kollipara, M. R. *J. Organomet. Chem.* **2004,** *689*, 3265.
32. Spectroscopic data for **1:** Chemical shifts (δ) are reported in parts per million (p.p.m.) and are referenced to the residual solvent peak. Coupling constants (*J*) are measured in Hz. ^{1}H

NMR (400 MHz, $CDCl_3$), 3.84 (3H, s), 3.88 (3H, s), 6.80 (1H, s), 6.85 (1H, dd, J_1=8.84, J_2=3.03), 6.98 (1H, d, J=8.84), 7.01 (2H, d, J=8.59), 7.17 (1H, d, J=3.03), 7.55 (2H, d, J=8.59); ^{13}C NMR (400 MHz, $CDCl_3$): δ=55.4, 56.0, 98.9, 111.5, 114.5, 114.7, 115.3, 117.6, 127.1, 152.6; mp: 146-150^{o}C; IR v_{max} (NaCl) 1508.4 cm^{-1}; MS (ES^+) m/z 297.05 (MH^+, 100%); HRMS (ES^+) $C_{17}H_{17}N_2O_3$ calc^{d}: 297.1234, obs^{d}: 297.1233.

33. Verdonk, M. L.; Cole, J. C.; Hartshorn, M. J.; Murray, C. W.; Taylor, R. D. *Proteins* **2003,** *52*, 609.

34. Sandy, J.; Holton, S.; Fullam, E.; Sim, E.; Noble, M. *Protein Sci* **2005,** *14*, 775.

35. Abuhammad, A. M.; Lowe, E. D.; Fullam, E.; Noble, M.; Garman, E. F.; Sim, E. *Protein and Cell* **2010,** *1*, 384.

36. Stauffer, S. R.; Coletta, C. J.; Tedesco, R.; Nishiguchi, G.; Carlson, K.; Sun, J.; Katzenellenbogen, B. S.; Katzenellenbogen, J. A. *J. Med. Chem.* **2000,** *43*, 4934.

37. Brooke, E. W.; Davies, S. G.; Mulvaney, A. W.; Pompeo, F.; Sim, E.; Vickers, R. J. *Bioorg. Med. Chem.* **2003,** *11*, 1227.

38. Campa, A.; Lazzeri, D.; Brafa, A.; Calabro, M.; Nisi, G.; Brandi, C.; D'Aniello, C. *J Plast Reconstr Aesthet Surg* **2009,** *62*, e155.

39. Pathak, R. B.; Chovatia, P. T.; Parekh, H. H. *Bioorg. Med. Chem. Let.t* **2012,** *22*, 5129.

Figure Legends

Fig. 1 Lead compound 4-methoxy-2-(5-(4-methoxyphenyl)-1*H*-pyrazol-3-yl)phenol **1**

Fig. 2 Predicted interactions of **1** with the NAT enzyme from *M. marinum* (MMNAT) and comparison of the binding site of **1** with the binding site of CoA, hydralazine and isoniazid in MMNAT. The protein is depicted in cartoon format and MMNAT, the residues that are predicted to interact with **1** are shown in stick format, the lead compound **1**, substrate and cofactor are shown in stick format. (a) Compound **1** was docked using GOLD and the residues that are predicted to interact with MMNAT are shown. The carbon atom's of **1** are depicted in magenta (b) The docking result of **1** is overlaid on the CoA-MMNAT structure (pdb 2vfc). The carbon atom's of CoA are depicted in yellow (c) The docking result of **1** is overlaid on the HDZ-MMNAT structure (pdb 3ltw). The carbon atom's of HDZ are depicted in cyan (d) The docking result of **1** is overlaid on the INH-MMNAT structure (pdb 1wf6). The carbon atom's of INH are depicted in grey.

Fig. 3 Surface representation of MMNAT docked with **1.** The molecular surface of the MMNAT protein is displayed and coloured to show hydrophobicity (red being most hydrophobic through to white to blue being most hydrophilic). The molecular surface of **1** is shown and carbon atom (green), oxygen (red), nitrogen (blue).

Fig. 4 Space filled representation of compounds **1**, **7, 8, 10** and **11**. The inhibitors are in the predicted docking orientation found in the active site pocket of MMNAT. (Carbon atoms (grey), oxygen atoms (red), nitrogen atoms (dark blue), fluorine atoms (light blue),

Fig. 5 Predicted binding interactions of compounds **7**, **8**, **10** and **11.** Compounds **7** (A), **8** (B), **10** (C) and **11** (D) were docked into the MMNAT protein (pdb code 2vfb) using the GOLD docking program. The compounds are shown in ball-and-stick format with the carbon atoms in magenta, nitrogen atoms in dark blue, oxygen atoms in red and the residues of MMNAT that are predicted to interact with the ligands are shown in stick format.

Scheme 1. Synthesis of **1**. *Reagents and conditions*: a) (i-iv): (i) LiHMDS, THF, -78^{o}C, (ii) -10^{o}C, (iii) 4-methoxybenzoychloride, RT, (iv) aq. work up, b) (v-vi): (v) $NH_2NH_2.xH_2O$, RT, (vi) H_2O).

Figure 1

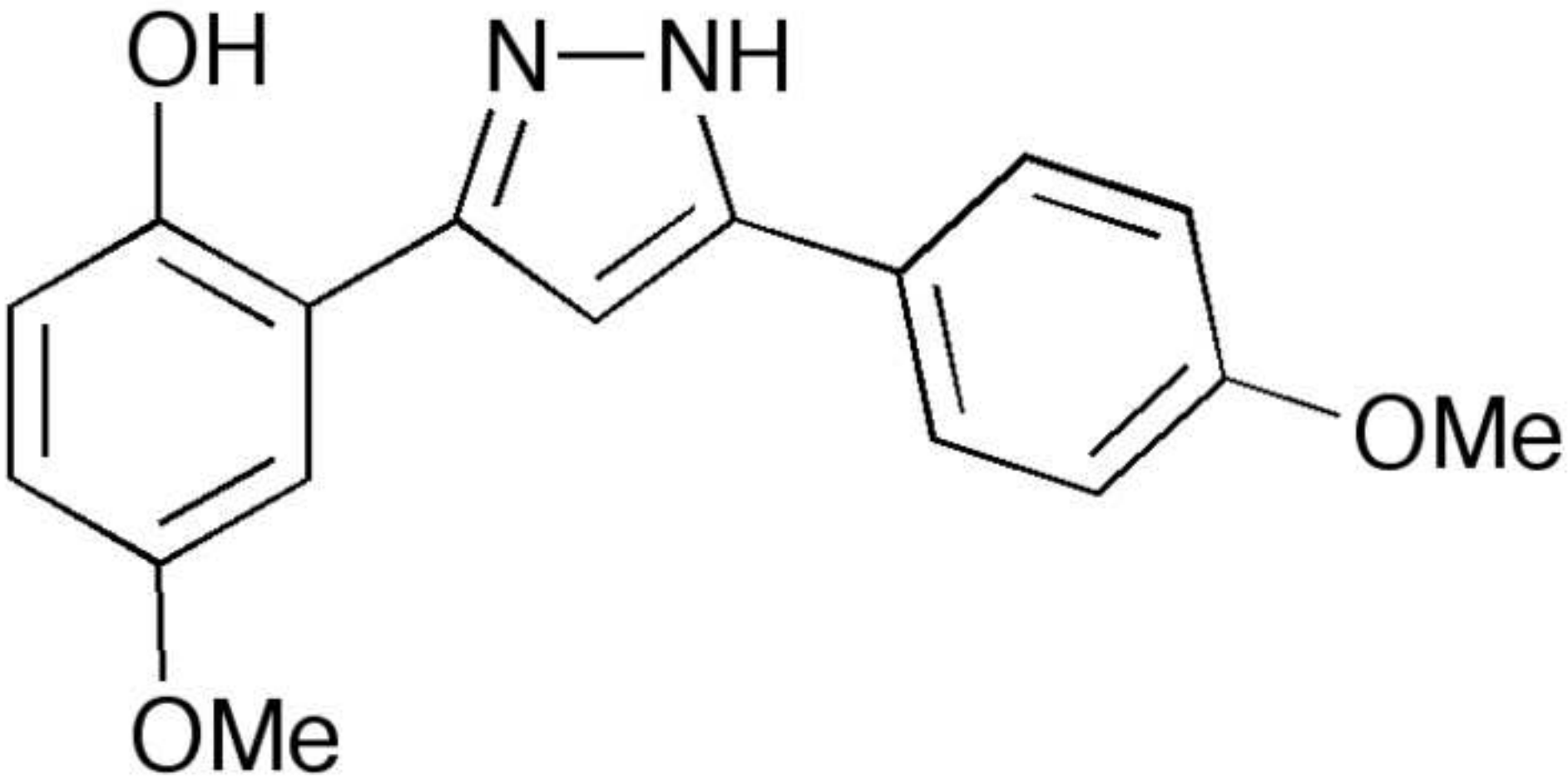

Figure 2

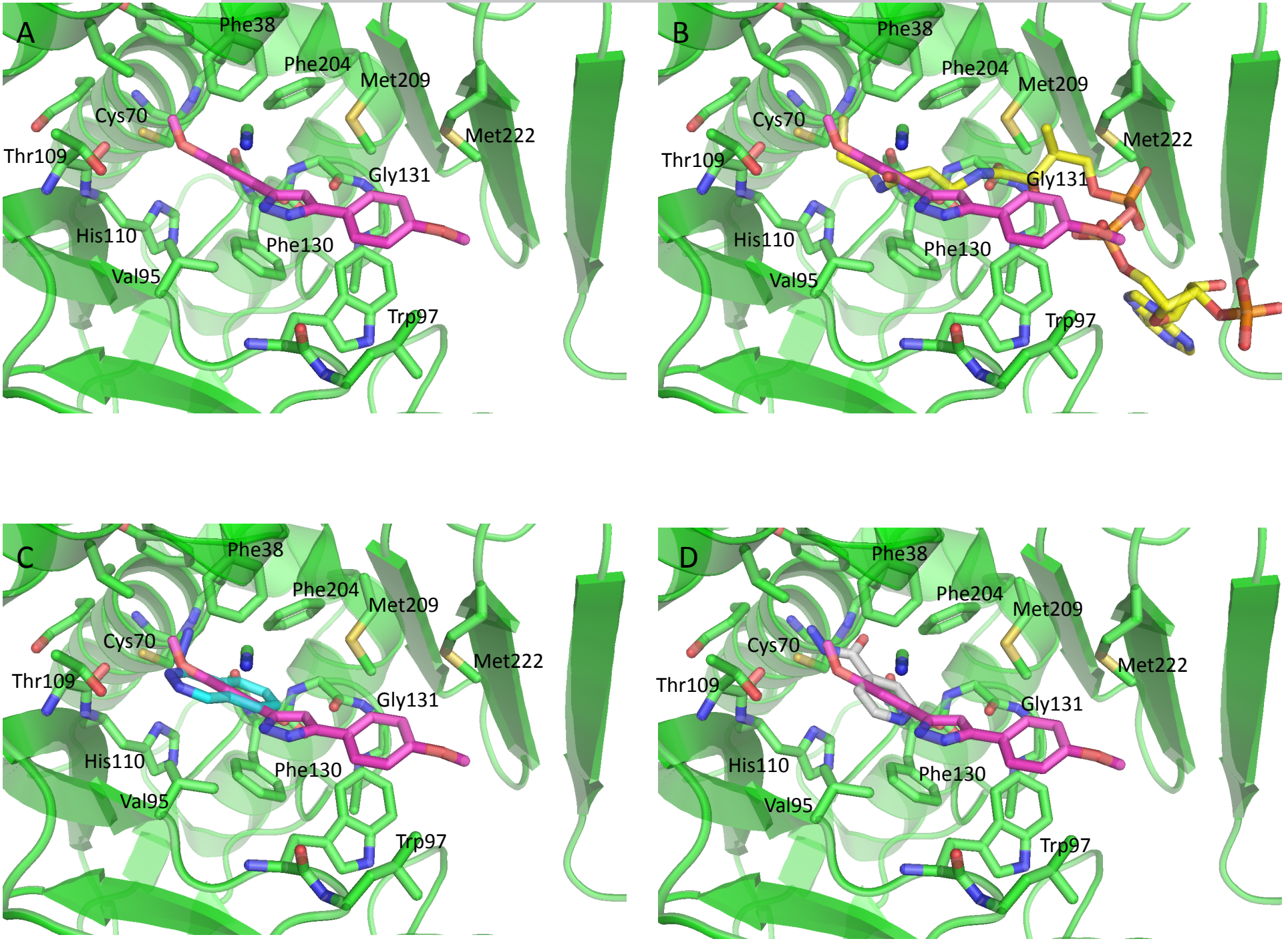

FIGURE 2

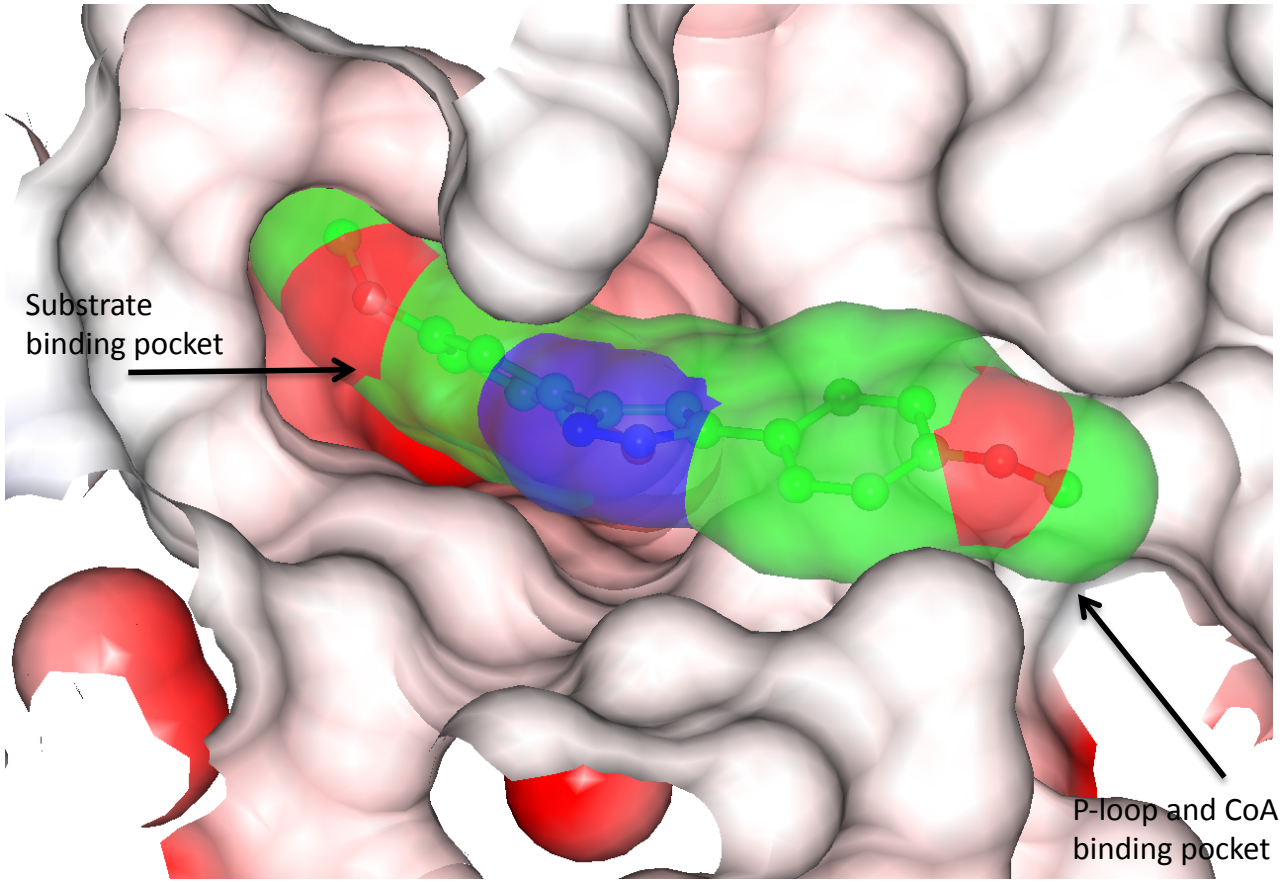

Figure 3

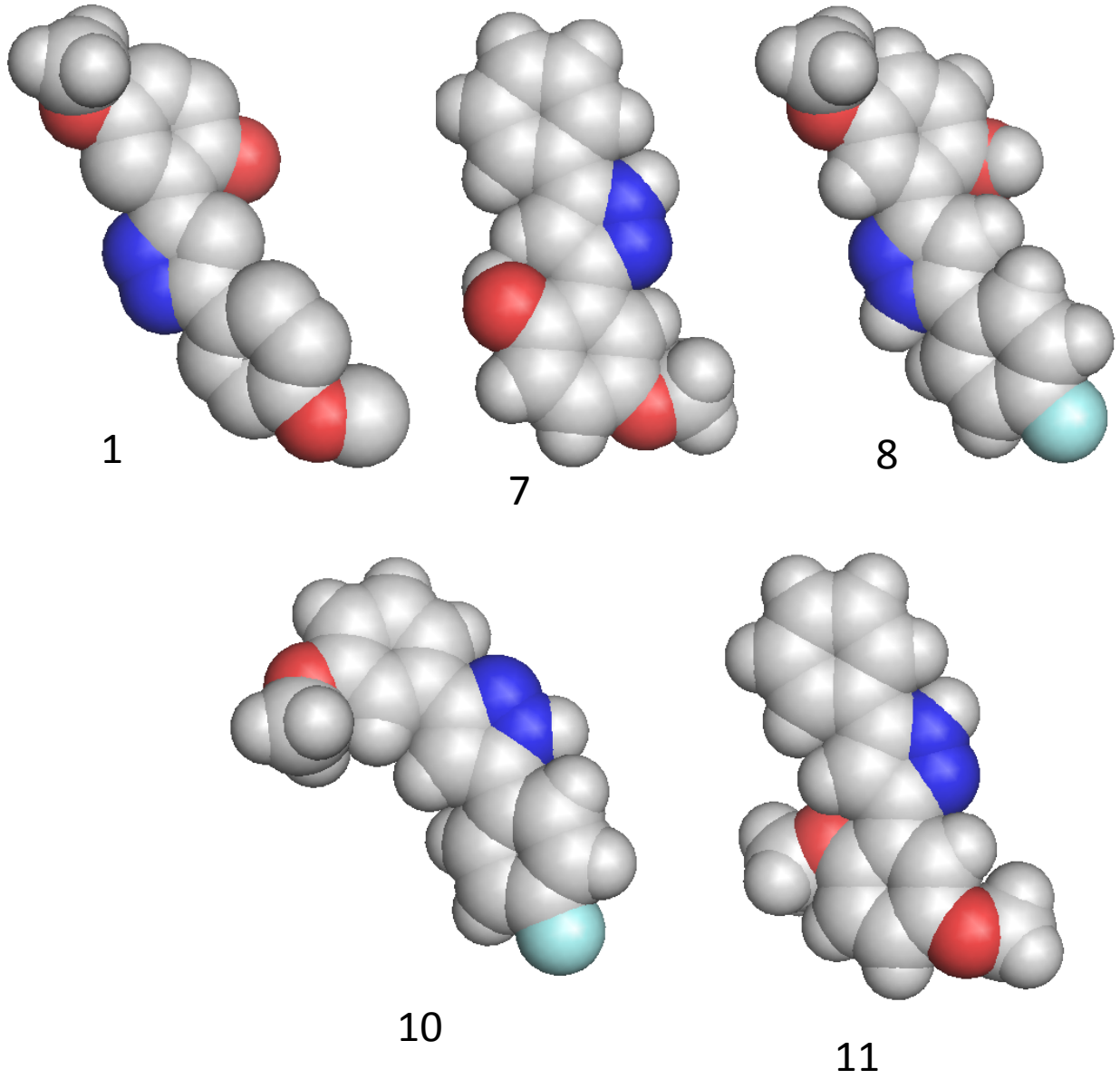

Figure 4

Figure 5

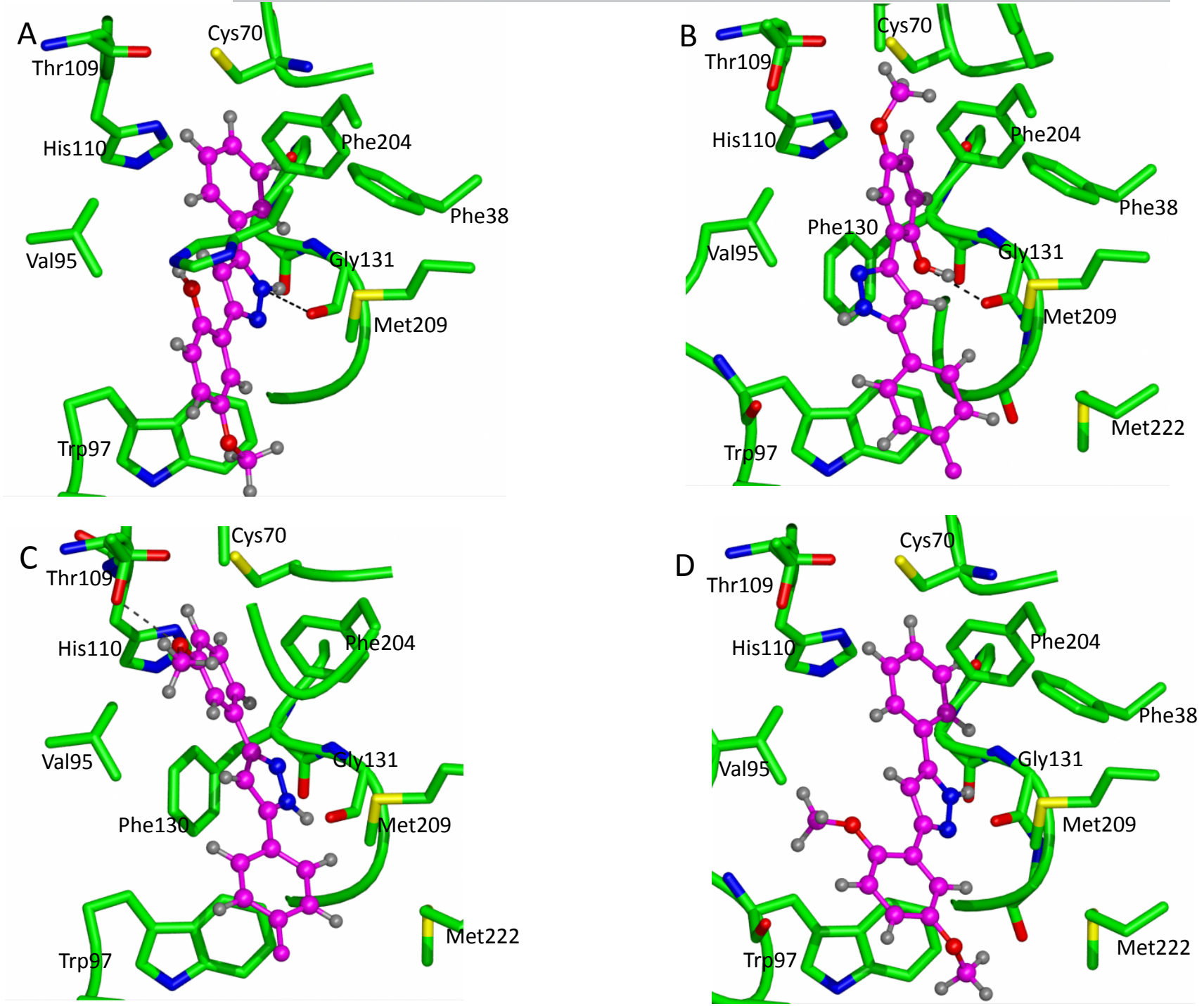

FIGURE 5

Scheme 1

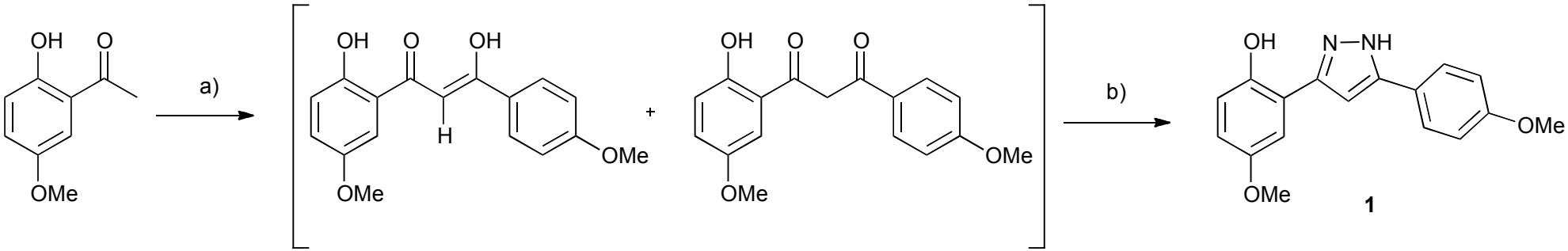

Scheme 1: reagents and conditions: i) LiHMDS, THF, -78°C, 1 hour, ii) -10°C, 2 hours, iii) 4-methoxybenzoylchloride, RT, 16 hours, iv) aq. work-up, v) $NH_2NH_2.xH_2O$ MeOH, RT, 15 minutes, vi) H_2O

Table 1. Biological activities of 3,5-diaryl-1*H*-pyrazoles with MMNAT

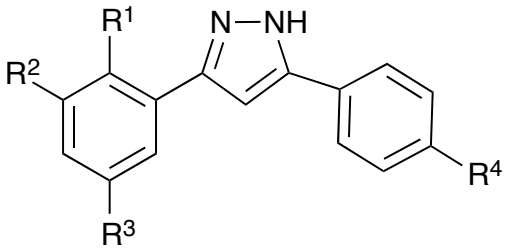

Compound	R^1	R^2	R^3	R^4	Overall Yield (%)[a]	clogP[b]	tPSA[b]	% Inhibition at 30μM[c]	IC_{50} (μM)[d]
1	-OH	-H	-OMe	-OMe	86	2.47	63.1	65.8±10.4	18.5 ± 1.0
2	-OMe	-H	-OMe	-OMe	85	2.79	52.1	29.2±6.1	>30
3	-OH	-H	-OH	-OMe	31	2.27	74.1	21.5±4.3	>30
4	-H	-OH	-OH	-OMe	24	1.84	73.8	15.6±4.8	>30
5	-H	-H	-H	-H	87	4.43	24.4	45.2±2.6	>30
6	-H	-H	-H	-OMe	91	4.46	33.6	26.5±5.9	>30
7	-OH	-H	-OMe	-H	58	3.6	63.1	53.9±5.5	12.9±1.0
8	-OH	-H	-OMe	-F	45	3.84	53.9	59.2±1.3	21.3±1.0
9	-H	-OMe	-H	-OMe	98	2.13	42.9	26.5±6.4	>30
10	-H	-OMe	-H	-F	40	2.34	33.6	61.2±4.3	17.6±1.0
11	-OMe	-H	-OMe	-H	89	2.75	42.9	50.7±3.0	11.7±1.0
12	-OH	-H	-F	-OMe	63	3.94	53.9	46.5±4.6	>30
13	-OH	-H	-F	-F	21	4.16	44.6	32.7±2.4	>30
14	-F	-H	-F	-H	10	3.64	24.4	53.5±4.6	18.8±.9
15	-F	-H	-F	-OMe	89	4.79	33.6	18.9±5.1	>30
16	-F	-H	-F	-F	81	4.93	24.4	29.7±4.8	>30

[a]Overall yield calculated over total synthetic steps starting from arylmethylketones. All compounds are >95% pure as determined by RP-HPLC.

[b]The calculated octanol/water partition coefficient: clogP and topological polar surface area: tPSA parameters were calculated in CS Chemdraw Ultra v12.0.2.

[c]Mean % inhibition ± standard deviation (n = 3), relative to a control as described in Materials and Methods.

[d] IC_{50}: Half-maximal inhibitory concentration against MMNAT

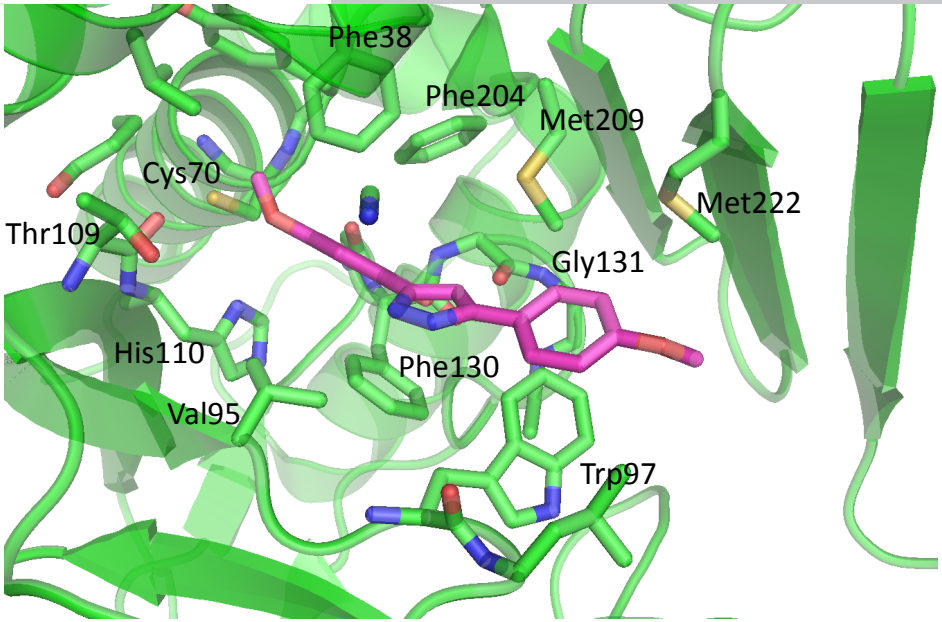
Phe38
Phe204
Met209
Cys70
Met222
Thr109
Gly131
His110
Phe130
Val95
Trp97

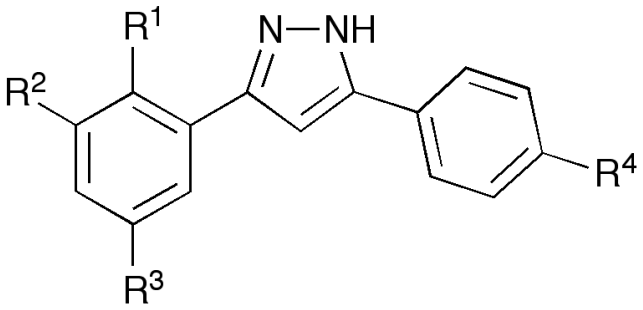
R1
N—NH
R2
R4
R3